


Article

Prediction of the Spatial Pattern of Carbon Emissions Based on Simulation of Land Use Change under Different Scenarios

Zhenhua Wu ¹, Linghui Zhou ^{1,*}  and Yabei Wang ²¹ Business School, Guilin University of Electronic Technology, Guilin 541004, China² Institute of Information Technology, Guilin University of Electronic Technology, Guilin 541004, China

* Correspondence: jessicanvi@163.com

Abstract: Land use is an important factor in the change of carbon emissions, and predicting the spatial pattern of carbon emissions under different land use scenarios is of great significance to respond to the “double carbon” target of China. Based on the land use data of Nanjing city, Jiangsu Province, China in 2010, 2015 and 2020, this study used the Conversion of Land Use and its Effects at Small regional extent (CLUE-S) model to simulate the land use change pattern in 2030 under multiple scenarios, and predicted the carbon emissions of each subzone based on the simulation results. It also provides a carbon balance zoning from an economic and ecological point of view and proposes strategies tailored to each district. The results show that: (1) in 2030, under the ecological conservation scenario, ecological land all shows different degrees of increase, while under the cultivated land conservation scenario, construction land only increased by 1.47%. This indicates that the ecological and cultivated land protection perspectives can effectively curb the expansion of construction land. (2) The growth rate of carbon emissions in Nanjing from 2010–2030 decreased from 16.65–3.7%. This indicates that carbon emissions continue to rise, but the trend of growth is slowing down. (3) The spatial carbon emissions in Nanjing show an overall higher level in the north and lower in the center; the large expansion of building land and the concentration of industrial industries are the main reasons for the large increase in carbon emissions. Under the ecological protection scenario, the carbon emissions of Lishui, Pukou and Qixia districts were 11.05×10^4 t, 19.437×10^4 t and 10.211×10^4 t lower than those under the natural growth scenario, mainly because these three districts have more ecological land and the ecological protection effect is more significant. Under the cultivated land conservation scenario, the growth rate of carbon emissions slows down significantly. This indicates that the future structure of carbon emissions in Nanjing will vary significantly, and that ecological protection and arable land conservation play an important role in reducing carbon emissions. This study shows that it is difficult to reduce emissions in a concerted manner. Therefore, for different districts, differentiated land use optimization measures should be developed according to local conditions, and ecological protection and cultivated land protection scenarios should both be taken into account.

Keywords: CLUE-S model; land use; carbon emission zoning; scenario simulation

Citation: Wu, Z.; Zhou, L.; Wang, Y. Prediction of the Spatial Pattern of Carbon Emissions Based on Simulation of Land Use Change under Different Scenarios. *Land* **2022**, *11*, 1788. <https://doi.org/10.3390/land11101788>

Academic Editors: Yanan Wang, Kees Klein Goldewijk, Wei Chen, Juan Wang and Xiaosong Ren

Received: 13 September 2022

Accepted: 11 October 2022

Published: 13 October 2022

Publisher's Note: MDPI stays neutral with regard to jurisdictional claims in published maps and institutional affiliations.



Copyright: © 2022 by the authors. Licensee MDPI, Basel, Switzerland. This article is an open access article distributed under the terms and conditions of the Creative Commons Attribution (CC BY) license (<https://creativecommons.org/licenses/by/4.0/>).

1. Introduction

In recent years, carbon emissions have attracted widespread international attention as the trend of global warming has further intensified. China has clearly proposed in 2020 to strive to achieve carbon peaking by 2030 and carbon neutrality by 2060. Carbon emissions caused by land use change have an important impact on global warming. Research shows that [1], since the industrial revolution, carbon emissions caused by land use change account for about one-third of the total carbon emissions from human activities. Yue et al. [2] concluded that the land carbon balance under human land use is composed of emissions from land use and land use change. They affirmed the importance of land use in the carbon cycle feedback and argued that to mitigate climate problems, the carbon sink capacity of land should be enhanced. Carbon emissions are not only directly related

to land use types, but also to geographical location, land management, and spatial and temporal patterns of land use [3]. Therefore, proposing low-carbon land use regulation countermeasures according to the carbon emission intensity of different types of land, and improving the spatial patterns of regional land use are of great significance to reduce carbon emissions, promote low-carbon development and cope with climate change [4].

The assessment methods of land use carbon emissions are divided into direct and indirect [5]. Direct carbon emissions refer to carbon emissions from land use itself, while indirect carbon emissions refer to carbon emissions caused by all human activities on different types of land. Scientific modeling of future spatial patterns of land use is essential to predict carbon emissions. At present, many models for simulating land use change exist, such as Markov chain prediction models, gray system models, etc. Additionally, in recent years, many scholars have coupled quantitative models for simulating and predicting land use change with spatial allocation algorithms and proposed many models for predicting spatial patterns of land use change, such as the meta cellular automata model (CA) [6], CLUE-S model [7], Geographical Simulation and Optimization Systems (GeoSOS) model [8], etc. Among them, the CLUE-S model is more widely used. The model is suitable for the simulation of small area land usage under different scenarios with fine resolution, which can better explain the spatial connection and relative stability between land use types and locations, and can be widely used in land use simulation [9].

Many studies have now explored the spatial and temporal characteristics and trends of land use carbon emissions at different scales, and discussed carbon emission efficiency, among others. Huang H et al. [10] explored the spatial and temporal evolution of land use carbon emissions, carbon sequestration and net carbon emissions in China's provinces from 2003–2016, and analyzed the equity and variability of carbon emissions through the Gini coefficient. Xia C et al. [11] proposed a land carbon correlation rate. The combined effects of urban land use changes on the carbon balance in Zhejiang Province during the periods 1995–2000, 2000–2005, 2005–2010 and 2010–2015 are discussed. They showed positive and negative land-related carbon conversions, as well as changes in ecological relationships. FAN Jianshuang et al. [12] measured and decomposed the carbon emission efficiency of different types of land use structures in 11 districts of Nanjing from 2005–2014. In these studies, the main focus was on carbon emission measurement and assessment, and the research area was gradually focused from larger scale range to a deeper small-scale area, which further improved the methodological system of carbon emission research. According to previous studies, the impact on land use change of carbon emissions mainly depends on the ecosystem type and land use type transformation. The related studies simulate the future land use change scenarios and their impact on carbon emissions based on the model, and provide suggestions for optimizing the land use structure with the goal of carbon balance. Yu Kangkang et al. [13] analyzed carbon emissions of different land use types in the Taihu basin during various historical periods and simulated land use and its carbon emissions for 2030–2040. Feng Y et al. [14] proposed a meta-automata model to predict land use scenarios and used these scenarios to estimate the total emissions in China and its changes from 2000 to 2030. Zhu W et al. [15] used a Markov-CLUE-S model to analyze land use changes in the Qihe watershed in the southern Taihang Mountains from 2005 to 2015. They predicted land use patterns and carbon stocks under natural growth, cropland conservation, and ecological conservation scenarios in 2025. However, in estimating the required area of land use types under different scenarios, only the probabilities were transferred by the modified Markov model without considering the relevant local policies. In summary, there is a wide range of research into carbon emissions based on land use change. The use of future scenario modeling to predict carbon emissions is also becoming more sophisticated. However, there is still a lack of zonal modeling of carbon emissions at a small scale. This includes providing a scientific basis for land use planning and decision-making in different regions based on the predicted results. Few studies have also taken into account relevant local policies when conducting scenario modeling.

Nanjing, as the capital of Jiangsu Province, is the core city of the Yangtze River Economic Belt and an important industrial base in China. With the rapid economic development, Nanjing's construction land has expanded rapidly and other types of land such as cultivated land and forest land have been shrinking, leading to soaring carbon emissions year by year. How to coordinate economic development and ecological civilization construction in the region has become a major issue. Rational planning of land use, and promoting green, low-carbon and high-quality development and green transformation of the city are conducive to providing a reference for emission reduction actions. This study simulated the spatial distribution of land use changes in 2030 based on land use data from 2010 to 2020. Combined with local policies, the spatial pattern of carbon emissions in 2030 was projected under three scenarios: natural growth, ecological conservation and cultivated land conservation. Carbon balance partitioning was carried out on the carbon emission projection results, and the differences in future carbon emission patterns between regions under different scenarios were analyzed.

2. Materials and Methods

2.1. Study Area

Nanjing city, Jiangsu Province, China (Figure 1) is located in the eastern part of China and the lower part reaches the Yangtze River, with a geographical location between $31^{\circ}14'$ and $32^{\circ}37'$ north latitude and $118^{\circ}22'$ and $119^{\circ}14'$ east longitude. Nanjing belongs to the subtropical monsoon climate, with four distinct seasons, abundant rainfall and good natural conditions. It is a hilly area, with low hills and gentle hills dominating, with low hills accounting for 3.5% of the total land area, hills for 4.3%, downland for 53%, and plains, depressions and rivers and lakes for 39.2%. At the same time, Nanjing is a fast-growing city with a high level of economization. It is an important gateway city of the Yangtze River Delta radiating the development of the central and western regions and an important node city of the strategic intersection of the eastern coastal economic belt and the Yangtze River economic belt. The city has a resident population of about 9,319,700 and a total area of 6587.02 km^2 [16].

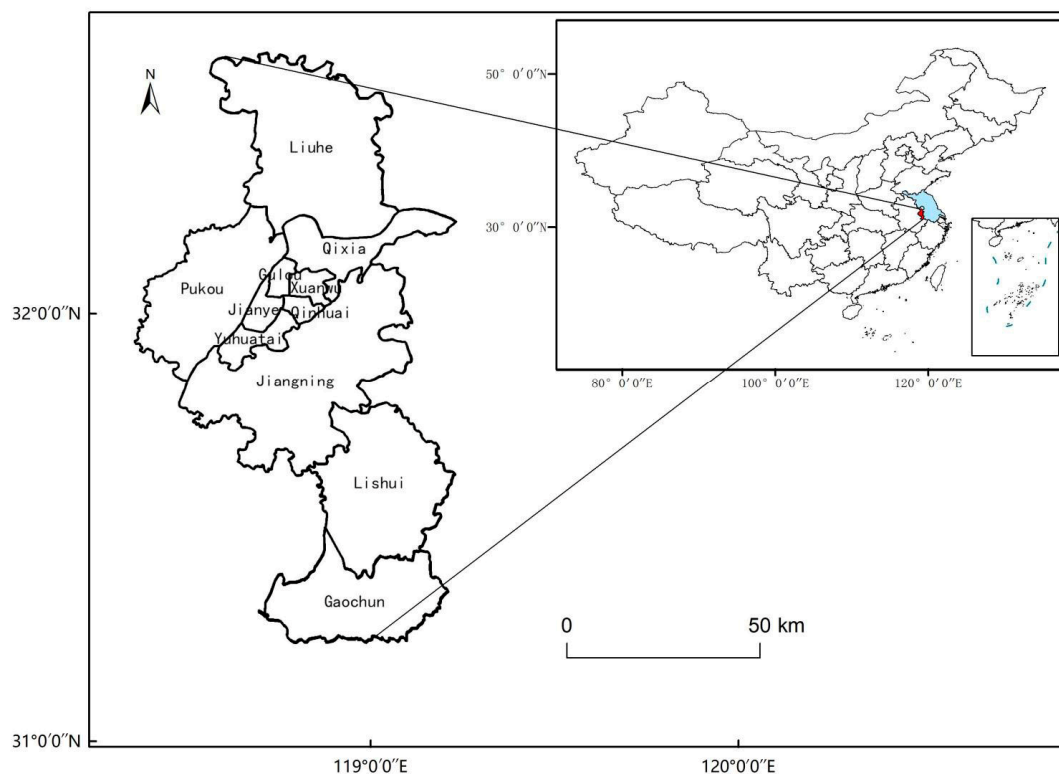


Figure 1. Location of Nanjing city in Jiangsu province of China.

2.2. Data Source and Processing

This study selected the land use remote sensing monitoring data of Jiangsu Province with a spatial resolution of 1 km for five periods of 2010, 2013, 2015, 2018 and 2020. We also used data of China's provincial administrative boundaries in 2015 and data of China's prefectural and municipal administrative boundaries in 2015. The above data are from the Resource and Environment Science Data Center of the Chinese Academy of Sciences (<http://www.resdc.cn>) (accessed on 24 July 2022). The natural environment data such as elevation and slope were obtained from the SRTM3 dataset in the geospatial data cloud (<http://www.gscloud.cn/>) (accessed on 28 July 2022) with a spatial resolution of 90 m. The spatial distribution of the population was obtained from WorldPop (<http://www.worldpop.org>) (accessed on 25 July 2022). The socio-economic data are represented by the nighttime lighting data of "Luoja-1" (<http://59.175.109.173:8888/index.html>) (accessed on 3 August 2022). Basic geographic information data, such as the spatial distribution of highways, railroads, rivers and lakes, were obtained from OpenStreetMap (<https://www.openhistoricalmap.org/>) (accessed on 26 July 2022). The spatial distribution data of protected areas include ecological protection areas, cultivated land and basic farmland restricted development areas in Jiangsu Province. They were obtained from *the National Ecological Protection Plan of Jiangsu Province* (http://www.jiangsu.gov.cn/art/2018/6/26/art_46143_7715521.html) (accessed on 23 July 2022) and *the General Land Use Plan of Jiangsu Province (2006–2020)* (http://g.mnr.gov.cn/201807/t20180720_2115893.html) (accessed on 23 July 2022) respectively. The data were imported into ArcGIS10.2 for geographic alignment and vectorization. The slope data were generated by the slope tool in ArcGIS based on the elevation data, and the distance elements such as distance from highway and distance from railroad were obtained by the Euclidean distance tool in ArcGIS. All data are unified in the coordinate system of CGCS2000_GK_CM_119E, and the resolution of all raster data was unified to 90 m by the resampling tool.

Economic and social indicators' data, energy and GDP data, etc., were obtained from *the Nanjing Statistical Yearbook* (<http://tj.nanjing.gov.cn/bmfw/njtjnj/>) (accessed on 5 August 2022) [16] and *the China Energy Yearbook* [17] for each year.

2.3. Research Methods

2.3.1. CLUE-S Model

This study used the CLUE-S model developed and improved by Verburg et al. [7] from Wageningen University & Research in The Netherlands. The model was developed to simulate land use change using the intrinsic quantitative and empirical relationships between land type change and drivers. It allows for relatively accurate spatial dynamic simulations at small scale scales based on different scenarios and top-down spatial allocation of land use type changes. The CLUE-S model is divided into two different modules, the non-spatial demand module and the spatial allocation module [18]. The non-spatial demand module, which needs to calculate the land use demand in the region according to the settings of different scenarios, usually relies on external models to accomplish this. In this study, Markov chains were used as an external prediction model to forecast the future land use quantity demand. The spatial allocation module is based on the theoretical foundation of where changes in a particular land class are most likely to occur. In this module, the probability of land use occurring at each location is calculated and the land use change is iterated year by year in conjunction with the land use demand. Thus, the spatial and temporal changes in future land use are simulated [18]. The principle of the CLUE-S prediction model is [19]:

$$TPROP_{i,u} = P_{i,u} + ELAC_u + ITER_u \quad (1)$$

where $TPROP_{i,u}$ is the probability of occurrence of land type u on grid i ; $P_{i,u}$ is the probability of spatial distribution calculated by the regression model; $ELAC_u$ is the elasticity coefficient of land use type u ; $ITER_u$ is the iterative variable of land use type u .

The following four components need to be considered as inputs to the CLUE-S model:

1. Logistic regression coefficient;

In this study, logistic regression was used to calculate the relationship between the distribution of land use types and the driving factors, linking the probability of land type occurrence with the location characteristics as a way to characterize the suitability of each area land type, which is often based on natural environmental, socioeconomic and other factors. Meanwhile, elevation, slope, slope direction, distance to rivers, and distance to lakes were selected as natural environmental factors, population density and nighttime lighting index as socio-economic factors, and distance to highway and distance to railway as transportation factors [20]. The logistic regression model can be written as following:

$$\log\left(\frac{P_i}{1-P_i}\right) = \beta_0 + \beta_1 X_1 + \beta_2 X_2 + \dots + \beta_n X_n \quad (2)$$

where P_i is the probability of occurrence of the specified land use type in a grid cell; X_n is each driver, i.e., independent variable; β_0 is the constant term; β_n is the coefficient of each independent variable.

A binary logistic regression model stepwise regression was constructed in IBM SPSS Statistics ver.25 software (Armonk, NY, USA: IBM Corp.) to achieve this, and the Receiver Operating Characteristic (ROC) method was adopted to assess the goodness of fit as a way to estimate the regression results [21]. Judging from the Area under the Curve (AUC) of the ROC, the value of AUC is between 0.5 and 1, and the closer to 1, the better the regression result.

Firstly, according to the land use remote sensing monitoring data from the Resource and Environment Science Data Center of the Chinese Academy of Sciences, the land use is divided into five categories: cultivated land, woodland, grassland, water body, and construction land. Because the amount of unused land is too small, this study classified the unused land into the category of construction land. The raster files of 5 land categories and 9 drivers were converted to ASCII files by the Raster to ASCII tool in ArcGIS. The single record file of each land category about 9 drivers was produced by using the convert software included in the CLUE-S model package, which was converted to an SPSS-applicable format and run SPSS for binary logistics. The results of the regression are shown in Table 1. The selected drivers have good fits for the five land categories of cultivated land, woodland, grassland, water body and construction land, with the values of AUC of 0.772, 0.781, 0.897, 0.805, 0.875, respectively.

Table 1. Logistic regression results.

Drive Factor	Cultivated Land	Woodland	Grassland	Water Body	Construction Land
Elevation	−0.003	0.055	−0.022	−0.0458	−0.009
Slop	−0.031	0.049	0.0236	−0.139	−0.002
Slope direction	0.009	−0.007	-	0.00024	-
Population density	−0.038	−0.0069	−0.00246	0.0033	0.049
Nighttime lighting index	−0.013	−0.01	0.00001	-	0.043
Distance to highway	0.00034	−0.0003	-	0.033	0.0512
Distance to railway	−0.009	−0.001	0.000033	0.024	0.0374
Distance to rivers	0.07	0.044	−0.000135	0.00059	0.097
Distance to lakes	0.01	0.096	−0.000087	-	0.174
Constant	−0.167	−1.047	1.492	0.42	0.6257

2. Land demand;

The Markov chain is a stochastic time series that uses the present state and movement of a variable to predict the future state of that variable and its movement [22]. Due to its excellent “memorylessness”, it is widely used in the simulation of land use demand quantities. The basic formula is shown below [23]:

$$S_{t+1} = P_{i,j} \times S_t$$

$$P_{i,j} = \begin{bmatrix} P_{1,1} & \cdots & P_{1,n} \\ \vdots & \ddots & \vdots \\ P_{m,1} & \cdots & P_{m,n} \end{bmatrix} \quad (3)$$

$$P_{i,j} \in [0, 1), \sum_{j=1}^n P_{i,j} = 1 (j, j = 1, 2, \dots, n)$$

where S_{t+1} and S_t are the number of each land use type at moments $t + 1$ and t , respectively; $P_{i,j}$ denotes the transfer probability matrix.

In this study, the Markov chain model was used to forecast the land use demand in 2030 based on the land use data in 2010 and 2020. The Markov model was also applied to obtain land use demand for 2023 based on data from 2013 and 2018, and 2027 based on data from 2013 and 2020. It was assumed that the speed of each category varies uniformly across the years 2020–2030, and the data for the remaining years were obtained using linear interpolation [15,24].

3. Transfer matrix and transfer elasticity;

The transition matrix indicates whether one land type can be converted into another land type; 1 means it can be converted, 0 means cannot be converted. The settings of the transition matrix are shown in Table 2.

Table 2. Land use transfer matrix.

Land Use Type	Cultivated Land	Woodland	Grassland	Water Body	Construction Land
Cultivated land	1	1	1	1	1
Woodland	1	1	1	1	1
Grassland	1	1	1	1	1
Water body	1	1	1	1	1
Construction land	1	1	1	1	1

The transfer elasticity was used to measure the reversibility of land use change, and its value is between 0 and 1; the closer to 0, the less likely the conversion will occur. According to the land use transfer matrix and transfer probability from 2010 to 2020, combined with expert experience, the transfer elasticity of cultivated land, woodland, grassland, water body and construction land under different scenarios was formulated (see Table 3). In the ecological protection scenario, in order to effectively protect the ecological land, the transfer of woodland, grassland and water bodies is increased, and the transfer elasticity of these three types of use is increased by 0.1. The transfer elasticity of cultivated land increased to 0.8.

Table 3. Transfer elasticity of land use types under different scenarios.

	Cultivated Land	Woodland	Grassland	Water Body	Construction Land
Natural growth scenario	0.6	0.7	0.7	0.8	0.9
Ecological protection scenario	0.6	0.8	0.8	0.9	0.9
Cultivated land protection scenario	0.8	0.7	0.7	0.8	0.9

4. Space policy and regional restrictions.

This part refers to the protected areas in the area where changes in land use are not allowed. According to the documents of *the National Ecological Protection Plan of Jiangsu Province* and *the General Land Use Plan of Jiangsu Province (2006–2020)*, this study made ecological protection restrictions area and cultivated land protection restricted area document respectively.

2.3.2. Accuracy Validation

The Kappa coefficient [25–27] is used as a measure of simulation accuracy. The value of the Kappa coefficient is between 0 and 1, and the closer to 1, the better the model simulation effect is. Generally, when the Kappa coefficient is greater than 0.75, it indicates that the simulation results are fitted better. The specific calculation formula is as follows:

$$\text{Kappa} = \frac{P_o - P_c}{1 - P_c} \quad (4)$$

where P_o is the ratio of the number of identical pixels in the simulated map to the total number of pixels in the actual utilization map, i.e., the proportion of correctly simulated pixels; P_c is the expected probability based on the consistency of the distribution of the simulated map.

2.3.3. Estimation of Carbon Emissions for Different Land Use Type

For the estimation of carbon emissions from different land types, there are two methods [28]. The first is the direct estimation method based on the Intergovernmental Panel on Climate Change (IPCC) inventory [29], where land use carbon emissions are calculated directly through carbon emission (carbon sequestration) factors. This method is applicable to areas with few human activities generating large amounts of carbon emissions, such as cropland, forest land, grassland, and water. The second one is to use the energy emission factor method in the IPCC report [30], and this method is applicable to construction land with large amount of human activities generating carbon emissions [31]. The carbon emission calculation formula for non-construction land is as follows:

$$E_k = \sum_{i=1}^4 e_i = \sum_{i=1}^4 e_i \times \delta_i \quad (5)$$

where E_k is the total direct carbon emission from non-construction land; i is the land use type; e_i is the carbon emission occurring on type i land; T_i is the total area of type i land; δ_i is the carbon emission or carbon absorption coefficient of type i land.

The carbon emission of cultivated land consists of the difference between carbon emission from conducting agricultural activities and carbon uptake by photosynthesis of crops on cultivated land, and the carbon emission factor of cultivated land was determined to be $0.0422 \text{ kg}/(\text{m}^2 \cdot \text{a})$ according to the study of Sun He et al. [32]. Woodland and grassland produce less carbon emissions from human activities and have better carbon sequestration capacity. The carbon emission coefficients of woodland and grassland were determined to be $-0.0631 \text{ kg}/(\text{m}^2 \cdot \text{a})$ and $-0.0021 \text{ kg}/(\text{m}^2 \cdot \text{a})$, according to Shi Hongxin et al. [33]. General water bodies include wetlands and lakes, which has better ecological conditions and is

mostly carbon sinks. The carbon emission factor of water body was determined to be $-0.0253 \text{ kg}/(\text{m}^2 \cdot \text{a})$ according to Shi Hongxin et al. [33].

Carbon emissions from construction sites are mainly composed of the sum of fossil energy consumption during production and construction and carbon emissions from population breathing. This study selected raw coal, washed coal, coke, natural gas, crude oil, gasoline, kerosene, diesel, fuel oil, and liquefied petroleum gas as the energy sources [12]. The formula for calculating carbon emissions from construction land is shown below:

$$E_t = \sum (E_{t1} + E_{t2})$$

$$E_{t1} = \sum_{i=1}^{10} E_{ti1} = \sum_{i=1}^{10} (E_{ti1} \times \theta_i \times f_i) \quad (6)$$

where E_t is the total carbon emissions from construction land; E_{t1} is the carbon emissions from the consumption of fossil energy for production activities; E_{t2} is the carbon emissions from population respiration; E_{ti1} is the carbon emissions from the consumption of fossil energy of category i ; E_{i1} is the total amount of fossil energy consumption of category i ; θ_i is the converted standard coal coefficient of fossil energy of category i ; f_i is the carbon emission coefficient of each type of energy.

According to the China Energy Statistical Yearbook and the IPCC Guidelines for National Greenhouse Gas Inventories, the Table 4 shows converted standard coal coefficients and the carbon emission coefficients of the 10 fossil energy sources.

Table 4. Fossil Energy Conversion Standard Coal Factor and Carbon Emission Factor.

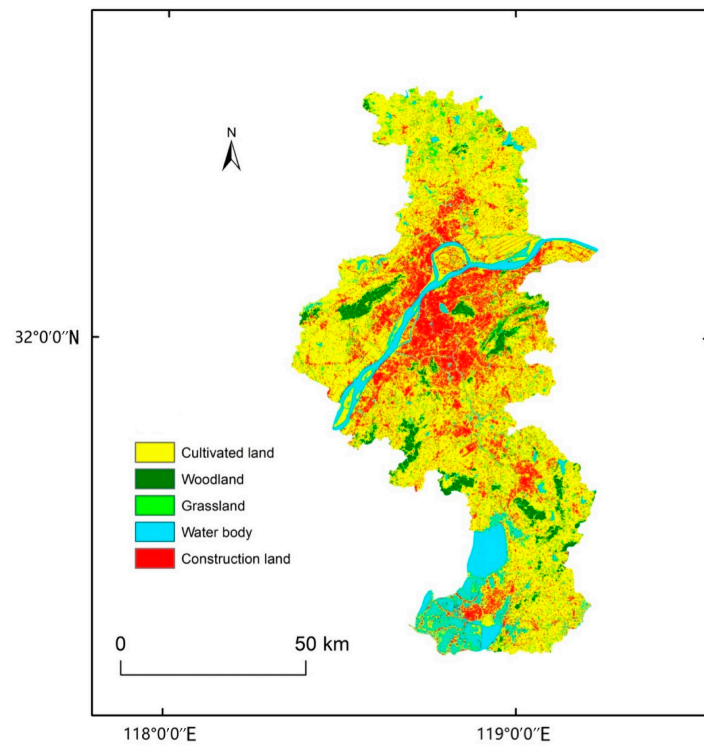
Energy	Discount Factor for Standard (Coalkgce/kg)	Carbon Emission Factor (t C/t)
Raw coal	0.7143	0.7559
Washed refined coal	0.9000	0.7559
Coke	0.9714	0.855
Natural gas	1.2143	0.4483
Crude oil	1.4286	0.5857
Gasoline	1.4714	0.5538
Kerosene	1.4714	0.5714
Diesel	1.4571	0.5921
Fuel oil	1.4286	0.6185
Liquefied petroleum gas	1.7143	0.5042

3. Results

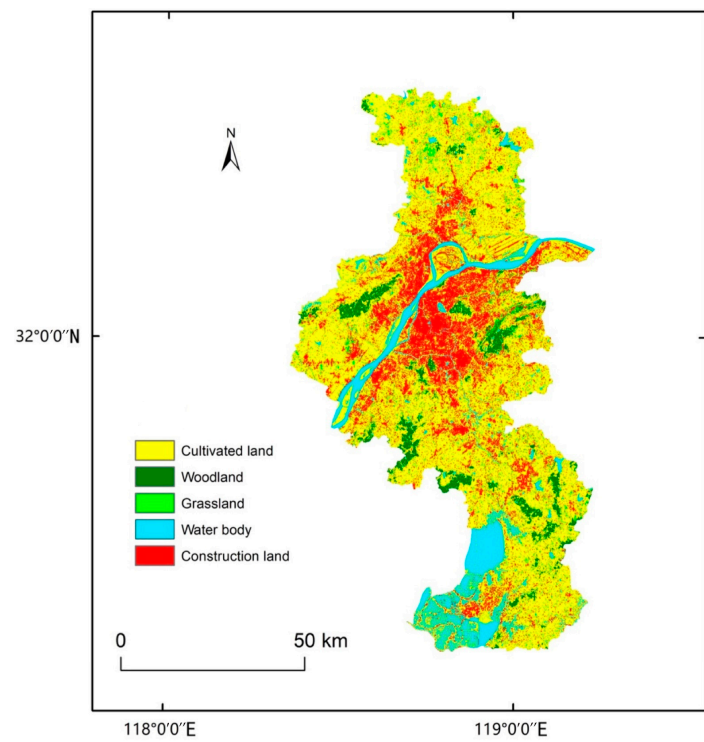
3.1. Simulation Accuracy Verification

Based on the land use data of Nanjing in 2010 and 2015, a Markov chain was applied to predict the land demand in 2020. The data for the missing years were obtained by linear interpolation. And all the data was input into the CLUE-S model to simulate the spatial structure of land use distribution in Nanjing in 2020. By comparing the real land use pattern in 2020 with the simulation results, the accuracy of the model and its applicability to this study area can be determined.

Using the two images as input data and applying the Kappa module in the Plus software accuracy verification, we can get the Kappa coefficient of simulated land use in Nanjing in 2020 as 0.8365, which is greater than 0.75; therefore, the CLUE-S model is considered to be able to predict the land use status better and with higher accuracy. Actual and simulated land use patterns in 2020 are shown in Figure 2.



(a) 2020's actual land use



(b) 2020's simulated land use

Figure 2. Comparison of actual land use and simulated land use in Nanjing in 2020.

3.2. Analysis of 2030 Land Simulation Results under Different Scenarios

For the current stage of development and future development needs of Nanjing, this study constructed three different scenarios of natural growth, ecological protection and cultivated land protection [34], and simulated the land use change pattern in 2030 under different scenarios by setting the number of growth or reduction of certain land types and adding different regional restriction files to the model [35].

3.2.1. Natural Growth Scenario

In the natural growth scenario, it was assumed that land use change from 2020–2030 is not constrained by spatial policies and regions and continues the natural evolutionary trend development from 2010–2020 without significant changes. This scenario is more common in land use change simulations and is one of the scenarios with high simulation accuracy in most studies [36,37]. The simulated land use pattern of Nanjing in 2030 under the natural growth scenario is shown in Figure 3.

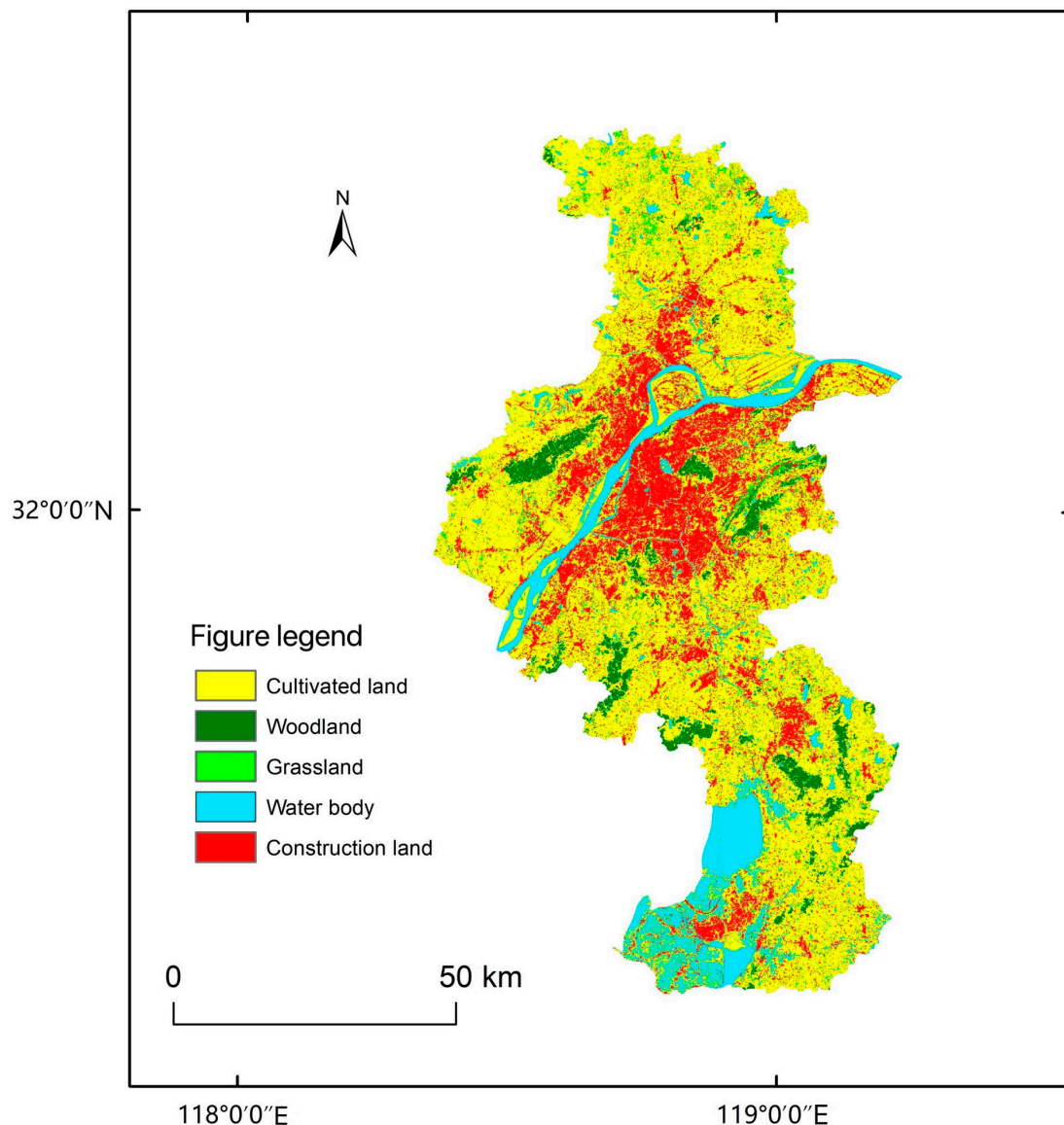


Figure 3. Spatial pattern of land use in Nanjing in 2030 under natural growth scenario.

In the period of 2020–2030, the areas of cultivated land, grassland and water will decrease by 14,575.95 hm², 625.32 hm² and 610.74 hm², and the areas of forest land and

construction land will increase by 413.1 hm² and 15,398.91 hm², respectively. By 2030, the cultivated land in Nanjing will decrease to 313,345.26 hm²; compared with 2020 it decreased by 4.44%. Grassland decreased to 5184 hm², a decrease of 10.76% compared to 2020, and water body decreased to 71,942.58 hm², a decrease of 0.84% compared to 2020. Woodland increased to 67,110.12 hm², an increase of 0.169% compared to 2020. Construction land increased to 190,192.05 hm², an increase of 8.81% compared to 2020. Under this trend, the increase of forest land and the decrease of water area are smaller, the area of cultivated land and grassland is significantly reduced, and the area of construction land is significantly increased. Construction is expanding at the cost of taking up cultivated land and grassland, and if the trend continues, it will cause a series of ecological and environmental problems.

From the spatial change pattern of land use in each district of Nanjing, the decrease of cultivated land area is concentrated in Jiangning District, Lishui District and Pukou District, with a decrease of more than 2000 hm². The increase of woodland area is mainly concentrated in Lishui District, Pukou District and Gaochun District; all three districts are located in the outer edge of Nanjing, far from the city center. Grassland area decreased in most areas, and only Pukou District had a small increase. The growth of water body is mainly concentrated in Lishui District, Liuhe District and Pukou District. The expansion trend of construction land is to grow outward along the existing large construction land and fill in the inner part of the city, at the cost of occupying a lot of cultivated land and other types of land. Since Lishui District, Gaochun District and Pukou District belong to the distant suburbs of Nanjing, the ecological environment is better; woodland, grassland and water bodies more or less increased. However, with the economic growth and accelerated urbanization in recent years, the construction land has expanded rapidly. The cultivated land areas in Jiangning District, Pukou District and Qixia District, where the increase of the construction land is most obvious, were all reduced by a large amount.

3.2.2. Ecological Conservation Scenario

Nanjing is the capital city of Jiangsu Province, and during the period of 2010–2021, the total economic volume crossed nine-hundred billion, achieving a historic breakthrough of one trillion, and ranking second in the GDP of 13 cities in Jiangsu Province. With the rapid development of the economy, problems such as the reduction of cultivated land area, the crowding of ecological space, and the shrinking of wetland area have come one after another. In order to make future development sustainable, this study designed an ecological protection scenario. Under this scenario, the amount of woodland, grassland and water body converted to construction land is reduced by 30%. The study also constructed a development restriction zone document based on *the National Ecological Protection Plan of Jiangsu Province*. Figure 4 shows the simulated land use pattern of Nanjing in 2030 under the ecological protection scenario.

Under the ecological protection scenario, compared with the land use in 2020, the areas of woodland, grassland, water body, and construction land increased by 2255.3 hm², 790.47 hm², 5255.33 hm², and 8199.45 hm², respectively, and the area of cultivated land decreased by 16,500.55 hm². Compared with the natural growth scenario, the areas of woodland, grassland, and water body increased by 1842.2 hm², 1415.79 hm², 5866.07 hm². The area of cultivated land and construction land decreased by 1924.6 hm², 7199.46 hm².

According to the spatial simulation pattern of land use, it can be seen that the woodland in Pukou District, Lishui District and Liuhe District has a more obvious growth. Grassland in Pukou District, Yuhuatai District and Liuhe District has a small growth. Larger waters such as Yangtze River, Shishu Lake and Gucheng Lake have a slight increase in water body size due to the surrounding ecological protection. The growth of the construction land area is concentrated in Pukou and Jiangning districts. Compared with the natural growth scenario in 2030, the ecologically relevant areas will grow by 9124.06 hm² under the ecological protection scenario. The most significant growth areas are Lishui District, Pukou District and Yuhuatai District, with an increase of 1914.30 hm², 1227.05 hm² and 1028.44 hm². From the overall pattern, except for the decrease of cultivated land,

the area of woodland, grassland and water bodies increased compared with the natural growth scenario, which indicates that the ecological protection scenario is beneficial to the ecological protection and sustainable development of Nanjing.

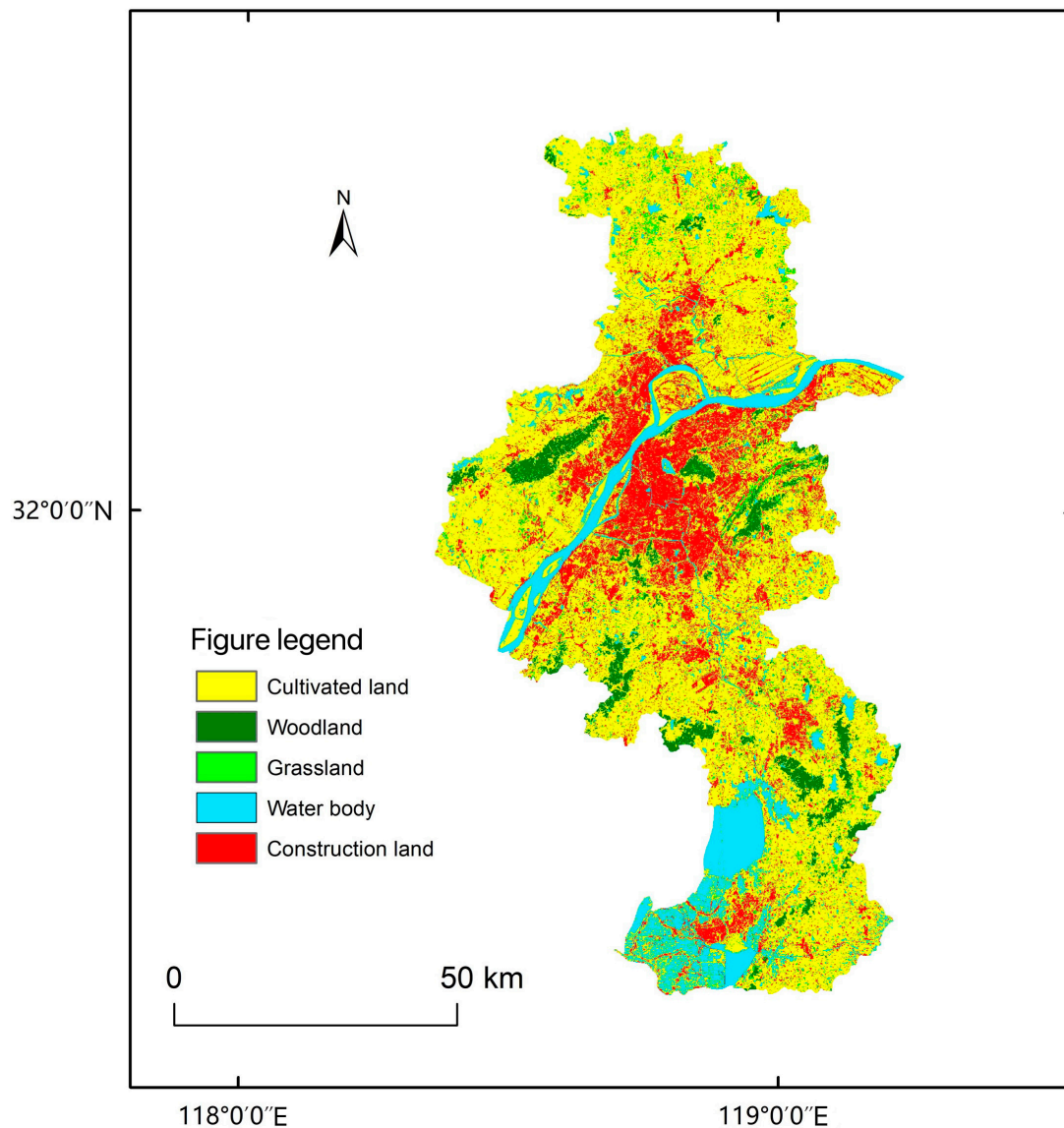


Figure 4. Spatial pattern of land use under ecological protection scenario in Nanjing in 2030.

3.2.3. Cultivated Land Conservation Scenarios

The rapid expansion of cities is accompanied by the crowding out of the quantity of high-quality cultivated land, which is a significant contradiction with the conservation of cultivated land, the quantity and quality of which are closely related to national food security [38]. In response to the national policy of cultivated land protection and to ensure national food security, this study designed a cultivated land protection scenario. Under this scenario, the conversion of cultivated land into construction land is reduced by 40%. The basic construction land is also set as a restricted area according to *the General Land Use Plan of Jiangsu Provincial (2006–2020)*. The simulation pattern of land use in 2030 under the scenario of cultivated land protection in Nanjing is shown in Figure 5.

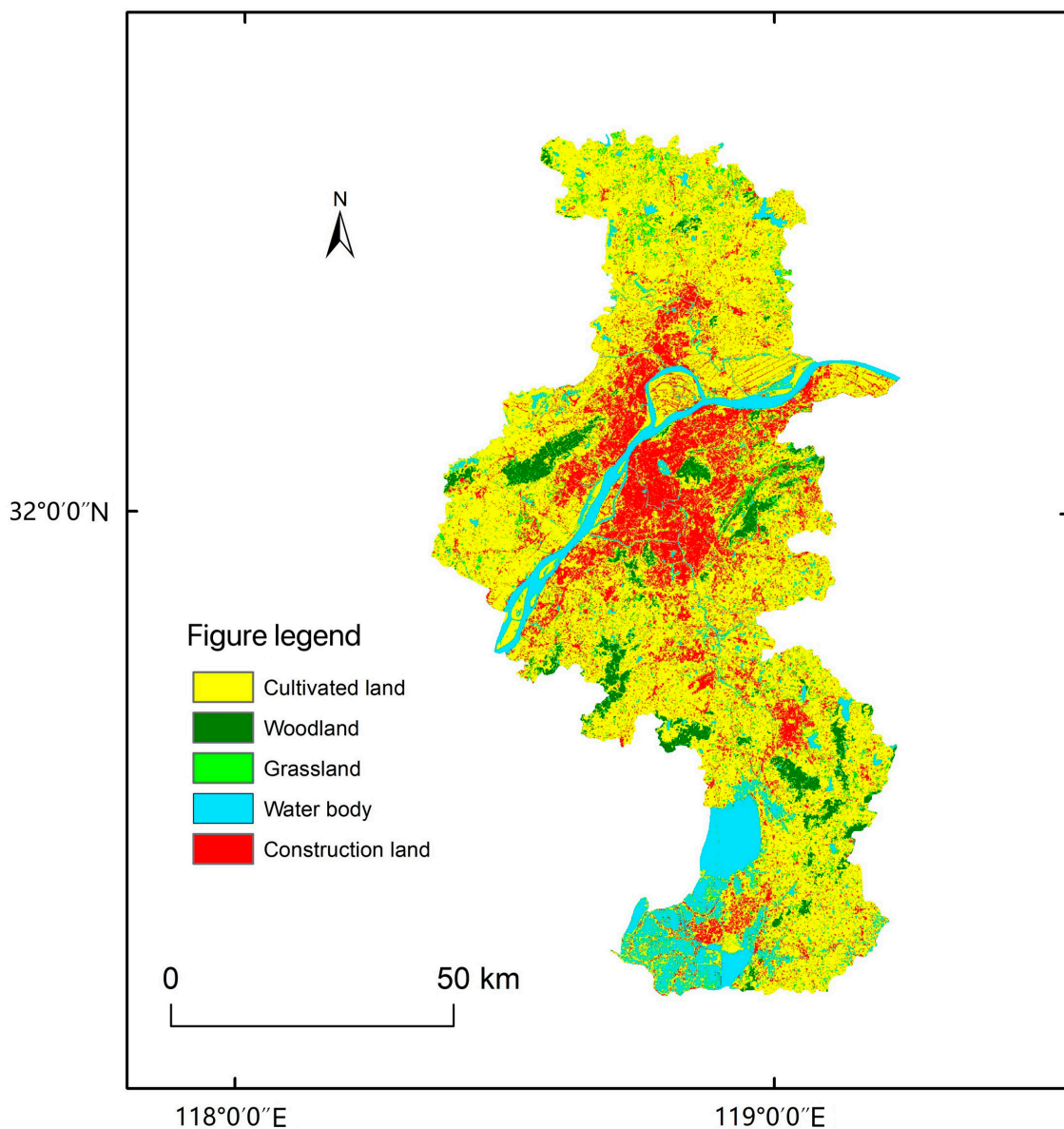


Figure 5. Spatial pattern of land use under cultivated land protection scenario in Nanjing in 2030.

Under the cultivated land conservation scenario, compared with the land use in 2020, the areas of woodland, grassland, water body and construction land increased by 1372.4 hm^2 , 94.16 hm^2 , 456.99 hm^2 and 3178.03 hm^2 , and the area of cultivated land decreases by 5101.58 hm^2 . Compared with the natural growth scenario, the areas of cultivated land, woodland, grassland and water body increased by 9474.37 hm^2 , 959.3 hm^2 , 719.48 hm^2 , and 1067.73 hm^2 , respectively, and the area of construction land decreased by 12,220.88 hm^2 .

According to the spatial simulation pattern of land use, it can be seen that a small amount of destruction of woodland occurred in Jiangning District, Liuhe District, and Gulou District, while all other areas grew. The change of grassland area is not obvious, with a small increase or decrease in several districts. The construction land in Lishui District, Liuhe District, Yuhuatai and Gaochun District all show a little negative growth; Jiangning District has a more obvious growth, and all other districts have a small growth. Compared with the natural growth scenario in 2030, the cultivated land area increased by 9474.37 hm^2 under the cultivated land conservation scenario. Cultivated land in Pukou, Liuhe, Lishui and Gaochun districts increased most significantly, with an increase of

1678.32 hm², 1485.27 hm², 1075.29 hm² and 960.16 hm², respectively. This is due to the fact that the cultivated land conservation areas are mainly set up in these four districts. From the overall pattern, the cultivated land increased the most. In the cultivated land restricted development area, besides the significant growth of cultivated land, the watershed is also relatively well protected, and the overall woodland, grassland and watershed areas have all increased to a certain extent, indicating that the cultivated land protection scenario has a certain effect on both cultivated land protection and natural ecological protection.

3.3. Carbon Emission Projections for Different Land Use Types

3.3.1. Trends in Carbon Emissions

The carbon emissions corresponding to each land use type are estimated below based on the simulated area of each land use type in 2030 under different scenarios (see Table 5). In this case, a linear regression model was developed to estimate the energy consumption and population density in 2030 based on the energy consumption and population density from 2010–2020. The results were used to calculate the carbon emissions of construction land in 2030 [13].

Table 5. Carbon emissions from different land categories in Nanjing, 2010–2030.

Year	Carbon Source (10 ⁴ t)			Carbon Sink (10 ⁴ t)			Total Carbon Uptake	Net Emission
	Cultivated Land	Construction Land	Total Carbon Emissions	Woodland	Grassland	Water Body		
2010	15.487	6164.065	6179.552	−4.26	−0.143	−1.808	−6.211	6173.341
2020	13.838	7193.661	7207.499	−4.209	−0.012	−1.836	−6.057	7201.442
2030's natural growth scenario	13.223	7460.864	7474.087	−4.235	−0.01	−1.82	−6.065	7468.022
2030's ecological conservation scenario	13.141	7412.538	7425.679	−4.351	−0.139	−1.969	−6.459	7419.22
2030's cultivated land conservation scenario	13.623	7395.295	7408.918	−4.295	−0.124	−1.847	−6.266	7402.652

According to the trend of carbon emission changes in each year, it can be seen that the carbon emission from 2010–2030 is on an increasing trend, from 6173.341×10^4 t in 2010 to 7201.442×10^4 t in 2020 and then to 7468.022×10^4 t in the forecasted 2030. The increase from 2020 to 2030 is 3.7%, and although the overall trend is still up, this is plateauing steadily. There are two main sources of carbon: cultivated land and construction land. The results show that the area of cultivated land is decreasing and the area of construction land is increasing every year. The reduction in carbon sources due to the reduction in the area of cultivated land is much smaller than the increase in carbon sources due to the increase in the area of construction land. This leads to a continuous increase in net emissions. The carbon sink effect of woodland is the largest, accounting for about 70% of the total carbon sink. Although the area of woodland in 2030 increased compared with 2020, it is still decreased compared with 2010, and the total absorption is on a decreasing trend, with a slight increase in 2030.

The main contributions of carbon sources and sinks come from construction land and woodland. However, due to the small area of ecological land, the carbon sources are much larger than the carbon sinks. Moreover, with the accelerated urbanization and industrialization of Nanjing in recent years, the population continues to gather in the city center area, fossil energy consumption is growing and construction land continues to expand. This has led to continued growth in net carbon emissions. If we do not protect ecological land and cultivated land, and limit the growth of energy consumption and area of construction land, it will lead to the unrestricted growth of carbon emissions and increased climate pressure. Under the two scenarios of ecological conservation and cultivated land conservation in 2030, there is a significant increase in the area of ecological land and a significant decrease in the area of construction land compared to the natural growth

scenario. Net carbon emissions decreased by 0.653% and 0.875%, compared to the natural growth scenario. This indicates that the adoption of ecological conservation or cultivated land conservation measures can effectively curb the growth of carbon emissions.

3.3.2. Spatial Patterns of Carbon Emissions

Table 6 shows the total net carbon emissions of 11 districts in Nanjing in 2020, under the natural growth scenario in 2030, the ecological protection scenario in 2030, and the cultivated land protection scenario in 2030. Among them, Jiangning District, Liuhe District and Pukou District have been in the first place in terms of carbon emissions. The total energy consumption is higher in these districts due to their large areas and significantly larger construction land areas than in other districts. In contrast, Qinhuai District, Jianye District and Xuanwu District have lower carbon emissions.

Table 6. Total Net Carbon Emissions by District in Nanjing.

Region	2020's	2030's Natural Growth Scenario	2030's Ecological Conservation Scenario	2030's Cultivated Land Conservation Scenario
Jianye	228.374	253.46	249.773	246.55
Jiangning	1904.852	1950.12	1942.472	1940.307
Lishui	484.752	474.493	463.443	472.09
Liuhe	1063.856	1078.836	1083.815	1083.224
Pukou	1014.747	1049.057	1029.62	1031.782
Qixia	768.749	804.273	794.062	783.531
Qinhuai	173.751	196.144	197.237	189.877
Xuanwu	269.47	300.071	310.173	299.749
Yuhuatai	248.473	276.189	269.891	270.641
Gaochun	344.936	358.02	348.005	355.843
Gulou	699.482	727.359	730.729	729.058

In order to distinguish the difference between carbon emissions of each district, Figure 6 has classified the 11 districts into three levels: light carbon emission, medium carbon emission, and heavy carbon emission. In 2020, Liuhe District, Pukou District, Qixia District, and Jiangning District are heavy carbon emission areas, Gulou District, Gaochun District, Lishui District, and Xuanwu District are medium carbon emission areas, and Jianye District, Yuhuatai District, and Qinhuai District are light carbon emission areas. In 2030, under the natural growth scenario, Jianye District changed from a light carbon emission area to a moderate carbon emission area, and Gulou District changed from a moderate carbon emission area to a heavy carbon emission area. Under the ecological protection and cultivated land protection scenario, the carbon emissions of each district decreased slightly due to a more or less reduction in the amount of land used for construction in all districts. The carbon emission classification of Jianye District remained unchanged and remained as a light carbon emission area.

Under the ecological protection scenario, carbon emissions in Lishui, Pukou and Qixia districts decreased the most, with 11.05×10^4 t, 19.437×10^4 t and 10.211×10^4 t, respectively. Gulou, Qinhuai and Xuanwu districts decreased the least. This indicates that the key areas for ecological protection are in the remote suburban areas at the edge of Nanjing, and that more ecological protection is needed in the city center. Under the cultivated land protection scenario, the carbon emissions in Pukou, Jiangning and Qixia districts all decreased more significantly, with 17.275×10^4 t, 9.813×10^4 t, 20.742×10^4 t, respectively, indicating that the cultivated land protection policy has a more significant effect on reducing carbon emissions. The cultivated land conservation scenario shows a greater decrease in carbon emissions per zone than the ecological conservation scenario. This is because the rate of reduction in construction land is greater than the rate of increase in cultivated land. Jiangning District ranks first in carbon emissions all year round, due to the presence of a large number of industrial enterprises in Jiangning District. It is also

one of the most important industrial clusters in Nanjing and has many energy-intensive industries.

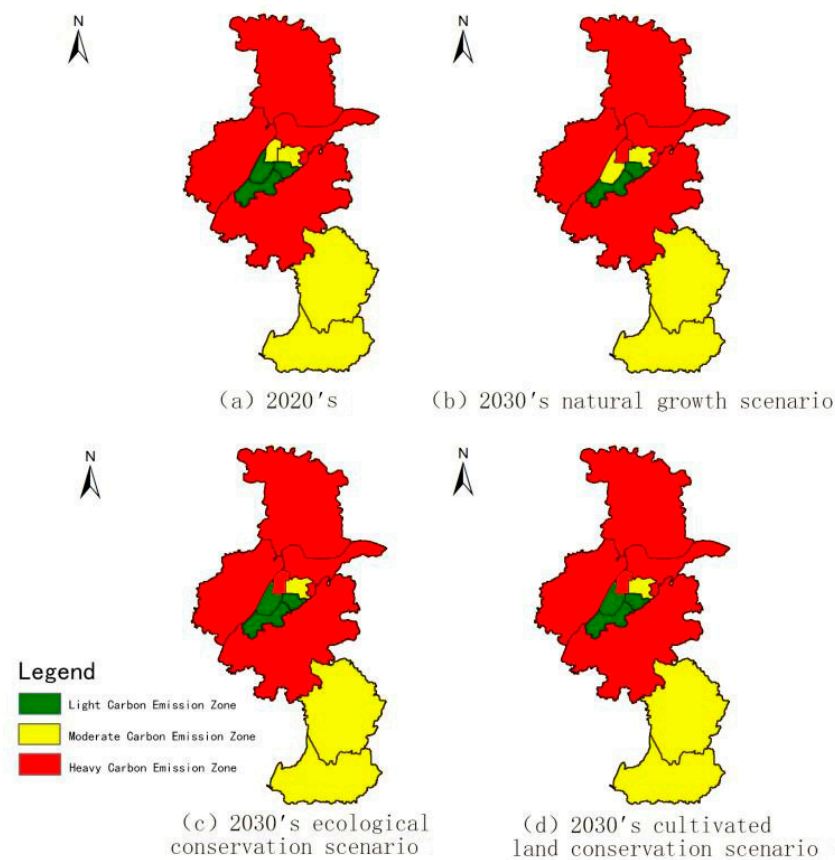


Figure 6. Spatial Distribution of Carbon Emissions by District in Nanjing under different scenarios from 2020 to 2030.

4. Discussion

In recent years, Nanjing's economy has been developing rapidly and the land use structure has been optimized, but the economic development is built on the basis of high input and high emission, and the carbon emission shows a rising trend. Therefore, it is important to adjust the economic development structure and realize the green and sustainable development of economy and ecology together.

Compared with the previous studies on land use scenario simulation, this study took relevant local policies into consideration, which will help to improve the accuracy of regional carbon emission estimation. To verify the accuracy of the method and model, this study used Markov chains to predict the demand in 2020 based on data from 2010 and 2015, and the remaining years were obtained by linear interpolation. The results were then input into the CLUE-S model for simulation. Then, we compared the mock-up with the real layout. The Kappa coefficient was 0.8365. Therefore, this study is reliable and reasonable in predicting carbon emission patterns by simulating land use with the CLUE-S model, indicating that the method is an effective method for predicting carbon emissions and carbon emission patterns.

Meanwhile, the zoning of the simulation results is conducive to the development of differentiated land use optimization measures according to the situation of different regions. The carbon balance zoning in this study focuses on the low carbon perspective, which can be used as a reference for collaborative emission reduction and development of a low carbon economy in the region. The main causes of increased carbon emissions differ between the regions delineated. For regions with different causes of carbon emissions,

differentiated low carbon development strategies can be proposed in a targeted manner to effectively improve the efficiency of emission reduction policies.

Cultivated land and construction land dominate in Nanjing, with the area of cultivated land decreasing and construction land expanding year by year. With the deepening of urbanization, carbon emissions are also rising year by year, but the prediction results show that the rising trend is slowing down and leveling off, and the carbon emission trend is more gentle under the ecological protection scenario and the cultivated land protection scenario; so, taking into account the cultivated land protection and ecological protection scenarios can achieve the carbon peak of land use faster. To achieve the future land use optimization target under the carbon peak and carbon neutral scenarios, the land use areas of different regions responding to the carbon peak were obtained based on the simulation results of zoning scenarios to optimize the land use pattern in Nanjing.

5. Conclusions

In this study, by simulating land use and projecting carbon emission zoning under different scenarios for Nanjing 2030, the following points are concluded:

- (1) The area of cultivated land, woodland and grassland in Nanjing will decrease by 10.49%, 0.89% and 20.55%, respectively from 2010 to 2020. The area of watershed and the area of construction land will expand, increasing by 1.26% and 28.32%, with construction land expanding significantly. In 2020–2030, under the natural growth scenario, cultivated land will continue to decrease and construction land will continue to expand; except for a small increase in woodland, the area of grassland and water body will both decrease; Under the ecological protection scenario, cultivated land will decrease by 5.03%, with ecological land showing varying degrees of reduction; Under the cultivated land protection scenario, cultivated land will decrease by 1.56%, while construction land will only increase by 1.47%, and the trend of decreasing cultivated land will slow down significantly. The simulation of different scenarios in 2030 shows that both the ecological protection scenario and the cultivated land restriction protection scenario can effectively restrain the rapid expansion of construction land and protect ecological areas.
- (2) Nanjing's carbon emissions will grow year by year from 2010 to 2030, but the growth trend is slowing down, from 6173.341×10^4 t in 2010 to 7201.442×10^4 t in 2020, and then to 7468.022×10^4 t in the forecasted 2030. The growth rate decreases from 16.65–3.7%. The carbon emissions are always much higher than the carbon absorption, with construction land as the main carbon source and forest land as the main carbon sink. Under the scenario of ecological protection and cultivated land protection, the carbon emissions are slightly decreased. Therefore, in the development process of Nanjing, it is important to focus on the protection of ecological land and cultivated land, slow down the expansion of construction land, and balance carbon sources and sinks in order to achieve carbon neutrality.
- (3) The overall carbon emission space of Nanjing is shown as higher in the north and lower in the center. Under the natural growth scenario, the areas with increased carbon emissions are significantly greater in number than those with decreased carbon emissions, mainly concentrated in Qixia, Pukou and Jiangning districts, with significant increases of 35.524×10^4 t, 34.31×10^4 t and 45.268×10^4 t. The large expansion of construction land and the gathering of industrial enterprises are the main reasons for the large increase of carbon emissions. In the ecological protection scenario, compared with the natural growth scenario, areas with reduced carbon emissions are more common than those with increased carbon emissions. Among them, Lishui District, Pukou District and Qixia District are the most significant, where carbon emissions are 11.05×10^4 t, 19.437×10^4 t and 10.211×10^4 t less than those in the natural growth scenario. Under the cultivated land protection scenario, the increase in carbon emissions slows down significantly, which is due to the significant decrease in the growth rate of the construction land area.

In summary, Nanjing's carbon emissions show a continuous rising trend from 2010 to 2020, but the rate of increase has slowed down. This rising trend continued under the natural growth scenario, while the ecological protection scenario can control the trend but cannot effectively control the reduction of cultivated land area, and the cultivated land protection scenario protects high-quality cultivated land while inhibiting the rapid expansion of construction land. Therefore, for the future optimization of land use structure in Nanjing, a balance should be struck between cultivated land protection and ecological protection scenarios. The expansion of construction land in Pukou District, Jiangning District, Qixia District and Liuhe District should be properly controlled, and the occupation of other types of land by construction land should be strictly controlled. Accelerate the adjustment of industrial structure and strengthen the protection of high-quality cultivated land. Additionally, researchers should carry out ecological restoration projects in Lishui District and Gaochun District to enhance the carbon sink capacity of the ecological carbon sequestration system. Meanwhile, we should give up low-quality cultivated land in Gulou District, Xuanwu District, Qinhuai District and Jianye District to ecological land to increase carbon storage. Food security and cultivated land quality will be ensured while achieving green and low-carbon sustainable development. Based on the results obtained, differentiated abatement strategies are proposed for each sub-district. This will promote efficient implementation of abatement actions according to local conditions, and provide a new perspective for the future sustainable ecological management of land and the formulation of green emission reduction measures in Nanjing.

Author Contributions: Conceptualization, Z.W. and L.Z.; Data collection, Z.W. and L.Z.; Methodology, L.Z.; analysis, Z.W., L.Z. and Y.W.; Writing-original draft, Z.W. and L.Z.; Writing-review & editing, Y.W. All authors have read and agreed to the published version of the manuscript.

Funding: National Natural Science Foundation of China, Research on the Value-added Process and Revenue Distribution of Urban Residential Land from the Perspective of Triadic Subjects, No. 71163008.

Data Availability Statement: Not applicable.

Acknowledgments: The authors would like to thank all the reviewers and editors for their professional suggestions and comments that have helped improve this paper.

Conflicts of Interest: The authors declare no conflict of interest.

References

1. Houghton, R.A.; Hackler, J.L. Emissions of carbon from forestry and land-use change in tropical Asia. *Glob. Chang. Biol.* **1999**, *5*, 481–492. [[CrossRef](#)]
2. Yue, C.; Ciais, P.; Houghton, R.A.; Nassikas, A.A. Contribution of land use to the interannual variability of the land carbon cycle. *Nat. Commun.* **2020**, *11*, 3170. [[CrossRef](#)]
3. Huang, B.; Hu, X.P.; Fuglstad, G.A.; Zhou, X.; Zhao, W.W.; Cherubini, F. Predominant regional biophysical cooling from recent land cover changes in Europe. *Nat. Commun.* **2020**, *11*, 1066. [[CrossRef](#)]
4. Xi, F.M.; Liang, W.J.; Niu, M.F.; Wang, J.Y. Carbon emissions and low-carbon regulation countermeasures of land use change in the city and town concentrated area of central Liaoning Province, China. *Chin. J. Appl. Ecol.* **2016**, *27*, 577–584.
5. Yang, J.; Zhang, M.; Duo, L.; Xiao, S.; Zhao, Y. Spatial Pattern of Land Use Carbon Emissions and Carbon Balance Zoning in Jiangxi Province. *Res. Environ. Sci.* **2022**, 1–14. [[CrossRef](#)]
6. Clarke, K.C.; Hoppen, S.; Gaydos, L. A self-modifying cellular automaton model of historical urbanization in the San Francisco Bay area. *Environ. Plan. B Plan. Des.* **1997**, *24*, 247–261. [[CrossRef](#)]
7. Verburg, P.H.; Soepboer, W.; Veldkamp, A.; Limpiada, R.; Espaldon, V.; Mastura, S.S.A. Modeling the Spatial Dynamics of Regional Land Use: The CLUE-S Model. *Environ. Manag.* **2002**, *30*, 391–405. [[CrossRef](#)] [[PubMed](#)]
8. Li, X.; Li, D.; Liu, X.P. Geographical simulation and optimization system (GeoSOS) and its application in the analysis of geographic national conditions. *Acta Geod. Cartogr. Sin.* **2017**, *46*, 1598–1608.
9. Verburg, P.H.; Eickhout, B.; Meijl, H.V. A multi-scale, multi-model approach for analyzing the future dynamics of European land use. *Ann. Reg. Sci.* **2008**, *42*, 57–77. [[CrossRef](#)]
10. Huang, H.; Zhou, J. Study on the Spatial and Temporal Differentiation Pattern of Carbon Emission and Carbon Compensation in China's Provincial Areas. *Sustainability* **2022**, *14*, 7627. [[CrossRef](#)]
11. Xia, C.; Chen, B. Urban land-carbon nexus based on ecological network analysis. *Appl. Energ.* **2020**, *276*, 115465. [[CrossRef](#)]

12. Fan, J.; Yu, X.; Zhou, L. Growth of carbon emission efficiency of land use structure in Nanjing and its spatial correlation. *Geogr. Res.* **2018**, *37*, 2177–2192.
13. Yu, K.; Wang, Y.; Sun, T.; Tian, J. Changes and Prediction of Carbon Emission from Different Land Use Types in Taihu Lake Basin. *Soils* **2022**, *54*, 406–414.
14. Feng, Y.; Chen, S.; Tong, X.; Lei, Z.; Gao, C.; Wang, J. Modeling changes in China's 2000–2030 carbon stock caused by land use change. *J. Clean Prod.* **2020**, *252*, 119659. [[CrossRef](#)]
15. Zhu, W.; Zhang, J.; Cui, Y.; Zhu, L. Ecosystem carbon storage under different scenarios of land use change in Qihe catchment, China. *J. Geogr. Sci.* **2020**, *30*, 1507–1522. [[CrossRef](#)]
16. Wang, G. *Statistical Yearbook of Nan Jing*; China Statistic Publishing House: Beijing, China, 2021; pp. 4–5.
17. Statistics Department, China National Bureau of Statistics. *The China Energy Yearbook*; China Statistics Press: Beijing, China, 2019; pp. 182–188.
18. Wang, L.; Zhang, X.; Zhang, H.; Wang, W. Principle and structure of CLUE-S model and its application progress. *Geogr. Geo-Inf. Sci.* **2010**, *26*, 73–77.
19. Verburg, P.H.; Schulp, C.J.E.; Witte, N.; Veldkamp, A. Downscaling of land use change scenarios to assess the dynamics of European landscapes. *Agric. Ecosyst. Environ.* **2006**, *114*, 39–56. [[CrossRef](#)]
20. Wang, H.; He, W. Lijiang River ecological interpretation of remote sensing of environmental change. In Proceedings of the International Conference on Remote Sensing, Environment and Transportation Engineering, Nanjing, China, 24–26 June 2011; pp. 442–445.
21. Pontius, R.G.; Schneider, L.C. Land use change model validation by an ROC method for the Ipswich watershed, Massachusetts, USA. *Agric. Ecosyst. Environ.* **2001**, *85*, 239–248. [[CrossRef](#)]
22. Yin, S.; Zhou, Y.; Pu, L.; Zhao, C.; Zhao, Y. Application of Markov chains in predicting land-use structure—an example from Wanbao Township, Loudi, Hunan. *Econ. Geogr.* **2006**, *31*, 120–123+130.
23. Cai, L.Y.; Wang, M. Effect of the thematic resolution of land use data on urban expansion simulations using the CA-Markov model. *Arab. J. Geosci.* **2020**, *13*, 120–123. [[CrossRef](#)]
24. Tang, J.; Yu, C.; Zhang, W.; Chen, D. Habitat quality assessment and prediction in Suzhou based on CLUE-S and InVEST models. *J. Environ. Eng. Technol.* **2022**, 1–13. Available online: <https://kns.cnki.net/kcms/detail/11.5972.X.20220325.1809.012.html> (accessed on 5 August 2022).
25. Pontius, R.G. Quantification error versus location error in comparison of categorical maps. *Photogramm. Eng. Remote Sens.* **2000**, *66*, 1011–1016.
26. KU, C.A. Incorporating spatial regression model into cellular automata for simulating land use change. *Appl. Geogr.* **2016**, *69*, 1–9. [[CrossRef](#)]
27. Yan, D.; Li, A.; Nan, X.; Lei, G.; Cao, X. The Study of Urban Land Scenario Simulation in Mountain Area Based on Modified Dyna-CLUE Model and SDM: A Case Study of the Upper Reaches of Minjiang River. *Geogr. Geo-Inf. Sci.* **2016**, *18*, 514–525.
28. Xia, T.; Wu, W.; Zhou, Q.; Verburg, P.H.; Yu, Q.; Yang, P.; Ye, L. Model-based analysis of spatio-temporal changes in land use in Northeast China. *J. Geogr. Sci.* **2016**, *26*, 171–187. [[CrossRef](#)]
29. National Greenhouse Gas Inventories Programme; Eggleston, H.S.; Buendia, L.; Miwa, K.; Ngara, T.; Tanabe, K. (Eds.) *2006 IPCC Guidelines for National Greenhouse Gas Inventories*; IGES: Kanagawa, Japan, 2006; Volume 4.
30. Boucher, O.; Randall, D.; Artaxo, P.; Bretherton, C.; Feingold, G.; Forster, P.; Kerminen, V.-M.; Kondo, Y.; Liao, H.; Lohmann, U.; et al. Clouds and Aerosols, Climate Change 2013: The Physical Science Basis. In *Contribution of Working Group I to the Fifth Assessment Report of the Intergovernmental Panel on Climate Change*; Stocker, T.F., Qin, D., Plattner, G.-K., Tignor, M., Allen, S.K., Boschung, J., Nauels, A., Xia, Y., Bex, V., Midgley, P.M., Eds.; Cambridge University Press: Cambridge, UK; New York, NY, USA, 2013; pp. 571–658.
31. Yang, X.; Ma, C.B.; Zhang, A.L. Decomposition of net CO₂ emission in the Wuhan metropolitan area of central China. *Sustainability* **2016**, *8*, 784. [[CrossRef](#)]
32. Sun, H.; Liang, H.; Chang, X.; Cui, Q.; Tao, Y. Land use patterns on carbon emission and spatial association in China. *Econ. Geogr.-Phys.* **2015**, *35*, 154–162.
33. Shi, H.; Mu, X.; Zhang, Y.; Lu, M. Effects of different land use patterns on carbon emission in Guangyuan city of Sichuan province. *Bull. Soil Water Conserv.* **2010**, *32*, 101–106.
34. Wu, Y.J.; Kong, X.S. Simulation and development mode suggestions of the spatial pattern of “ecology–agriculture–construction” land in Jiangsu Province. *Remote Sens. Nat. Resour.* **2022**, *34*, 238–248.
35. Fan, W.; Dai, X.; Xie, Y.; Gao, Y. Prediction and analysis of land use change in sichuan province in the next 10 years based on CLUE-S model. *Sci. Technol. Eng.* **2022**, *22*, 2641–2647.
36. Xiang, S.; Wang, Y.; Deng, H.; Yang, C.; Wang, Z.; Gao, M. Response and multi-scenario prediction of carbon storage to land use/cover change in the main urban area of Chongqing, China. *Ecol. Indic.* **2022**, *142*, 109205. [[CrossRef](#)]
37. Cui, X.; Liu, Y.; Guo, Y.; Li, S.; Hu, Y.; Zhang, F.; Wang, L. Simulation of land use change zoning based on geographically weighted CLUE-S model. *Jiangsu Agric. Sci.* **2019**, *47*, 287–293.
38. Zhong, T.; Huang, X.; Chen, Y. Evaluation of the Effectiveness of Cultivated Land Protection by Basic Farmland Protection Policy. *China Popul. Resour. Environ.* **2012**, *2*, 90–95.